Marginal zone macrophages suppress innate and adaptive immunity to apoptotic cells in the spleen

*Tracy L. McGaha,[1] *Yunying Chen,[2] Buvana Ravishankar,[1] Nico van Rooijen,[3] and Mikael C. I. Karlsson[2]

[1]Department of Medicine, Immunotherapy Center, Georgia Health Sciences University, Augusta, GA; [2]Department of Medicine, The Karolinska Institute, Stockholm, Sweden; and [3]Department of Cell Biology and Immunology, Free University, Amsterdam, The Netherlands

Marginal zone macrophages (MZMs) are a small subset of specialized splenic macrophages known to interact with apoptotic material entering the spleen from circulation. To evaluate whether MZMs regulate immunity to apoptotic material we depleted MZMs and assessed innate and adaptive immune responses to apoptotic cells administered systemically. MZM depletion altered the spatial localization of apoptotic cells, which accumulated in T-cell areas of the lymphoid follicles. MZM depletion also enhanced phagocytosis of apoptotic cells by red pulp ($CD68^+F4/80^+$) macrophages, which expressed increased CD86, MHCII, and CCR7. MZM depletion led to increased production of proinflammatory cytokines and enhanced lymphocyte responsiveness to apoptotic cell antigens. Furthermore, we found that MZM depletion accelerated autoimmune disease progression in mice genetically prone to systemic lupus erythematosus and caused significant mortality in wild-type mice repeatedly exposed to exogenous apoptotic thymocytes. These findings support the hypothesis that MZMs are central in the clearance of apoptotic cells to minimize the immunogenicity of autoantigens. (*Blood*. 2011;117(20): 5403-5412)

Introduction

The marginal zone (MZ) of the spleen represents the boundary between the lymphoid white pulp (WP) and the more innate scavenging red pulp (RP).[1] Most arterial blood entering the spleen passes through the MZ where it interacts with nonmotile macrophages tightly bound to the reticulum.[2,3] These macrophages line the marginal sinus and are defined by differential expression of macrophage scavenger receptor **MA**crophage **R**eceptor with a **CO**llagenous structure (MARCO).

The MZ is essential for trapping of particulate antigen, and MZ macrophages (MZMs) in particular have been implicated in this function.[4] $MARCO^+$ macrophages are well equipped for this because they express an array of scavenger receptors in addition to MARCO, including scavenger receptor A (SR-A) and SIGNR1 (a mouse homologue of DC-SIGN). Moreover, $MARCO^+$ macrophages are thought to be essential in the response to several blood-borne pathogens,[4-7] and studies have indicated mice deficient in MZMs are more susceptible to infection with altered T-cell response to antigenic challenge.[4,6]

The importance of MZMs in the clearance of endogenous material is less clear. SR-A and MARCO bind to acetylated and oxidized low-density lipoprotein and polyanionic ligands.[8,9] Moreover, both scavenger receptors aid in capture and phagocytosis of apoptotic cells by macrophages in vitro, suggesting an involvement in MZ-mediated retention of apoptotic material.[10,11] Curiously, deletion of either receptor has no apparent effect on apoptotic cell clearance in vivo,[12] probably reflecting mechanistic redundancy. However, we have demonstrated that apoptotic cell injection in SR-A/MARCO double knockout (KO) mice led to increased production of anti-dsDNA antibodies whereas injection in wild-type, SR-A, or MARCO single KO mice had no effect.[11] Further, in murine lupus MARCO expression is associated with defects in apoptotic cell phagocytosis and autoimmunity.[13]

Systemic apoptotic cell administration leads to suppression of immune responsiveness to apoptotic cell–associated antigens. Although the mechanisms behind this response are not well understood, it probably involves multiple components.[14-16] As systemically administered apoptotic cells are targeted to the MZ and are ingested by MZMs, MZMs may play a role in apoptotic cell antigen-specific suppression. Supporting this, Miyake et al[17] reported that deletion of MZMs compromised the ability of apoptotic cells to suppress autoimmunity in experimental autoimmune encephalitis.

This begs the question of the role of MZMs in peripheral homeostasis. Evidence suggests alterations in the ability of phagocytes to capture or clear apoptotic cells results in autoimmunity.[18-21] Thus, handicapping recognition/removal of cellular debris may be a fundamental defect in the development of autoimmune diseases. Because MZMs are probably important for initial interactions with apoptotic cells, we hypothesized that they may be relevant in maintaining homeostasis in the periphery. To test this we used a strategy to deplete MZMs by the administration of low-dose clodronate liposomes (CLs).[4] In MZM-depleted animals we examined apoptotic cell trafficking within the spleen as well as the effect on autoimmunity in lupus-prone and wild-type animals. Our results suggest that MZMs play an important role in how apoptotic cell-associated antigens are processed within the spleen and in the regulation of systemic immunity to self.

Submitted November 19, 2010; accepted March 12, 2011. Prepublished online as *Blood* First Edition paper, March 28, 2011; DOI 10.1182/blood-2010-11-320028.

*T.L.M. and Y.C. contributed equally to this study.

The online version of this article contains a data supplement.

The publication costs of this article were defrayed in part by page charge payment. Therefore, and solely to indicate this fact, this article is hereby marked "advertisement" in accordance with 18 USC section 1734.

Methods

Mice

Female C57BL6/J (B6), B6.Act-mOVA-II (Act-mOVA), B6.*cd45.1*$^+$, and B6.OTII (OTII) mice 8-12 weeks of age were obtained from The Jackson Laboratory. Female B6.*fcgr2b*$^{-/-}$ mice were provided by Dr Jeffrey Ravetch (The Rockefeller University). All mice were maintained under specific pathogen-free conditions at the animal facilities of the Georgia Health Sciences University in accordance with institutional and Institutional Animal Care and Use Committee guidelines, and all animal studies were approved by The Georgia Health Sciences University Institutional Animal Care and Use Committee.

Apoptosis induction and in vivo apoptotic cell/microparticle administration

For the generation of apoptotic cells, thymocytes collected from 8-week-old female B6 or Act-mOVA mice were exposed to 2000 cGy of radiation and cultured for 6 hours at 37°C in RPMI 1640 media plus 1% BSA (Sigma-Aldrich). Annexin V and propidium iodine staining confirmed apoptosis induction and showed that typically $> 85\%$ of the thymocytes were apoptotic with $< 1\%$ of the cells necrotic (data not shown).

For in vivo administration of apoptotic cells mice were injected intravenously with 10^7-10^8 apoptotic thymocytes. In one set of experiments 4 and 18 hours after administration of 5×10^7 apoptotic cells the sera were collected for assessment of serum IFN-γ, IL-6, IL-10, IL-12, IL-13, TNF-α, and IL-17 by multiple parameter Luminex assay, and the spleens were removed for histologic analysis. TGF-β1 levels were determined by ELISA (eBioscience). In CL-treated groups mice were injected with the indicated amounts of clodronate-impregnated or an equivalent amount of PBS-loaded control liposomes (PBSLs) in a final volume of 200 μL prepared as described 48 hours before administration of apoptotic cells.[22]

In another set of experiments mice were injected with liposomes as described earlier 1 time per week and 10^7 apoptotic thymocytes in 200 μL of PBS intravenously 2 times a week for a period of 5 months. The mice were assessed for αdsDNA autoantibody development as described below monthly by retro-orbital eye bleed.

Autoantibody detection

Assays for serum autoantibodies have been described previously.[23] Briefly, Immulon II plates (Dynatech) precoated with BSA were coated with 50 μg/mL calf thymus dsDNA (Sigma-Aldrich). To assay for serum autoantibody levels 100 μL of whole blood was collected from mice by retro-orbital bleed, and the serum was separated with the use of blood collection micro tubes (Sarstedt). The serum was diluted and assayed for autoantigen reactivity against the plates described above by incubation for 2 hours at room temperature. Bound IgG was detected with a goat polyclonal HRP–anti-mouse IgG detection antibody (Bethyl Laboratories) and visualized at 450 nm with the use of TMB substrate (Sigma-Aldrich). Total serum IgG was determined by a mouse IgG quantification ELISA (Bethyl Laboratories).

Antinuclear antibody (ANA) tests were performed on Hep-2 12-well slides (Bion) stained with mouse serum at a 1:200 dilution in PBS plus 1% BSA for 30 minutes followed by a 1:200 dilution in PBS plus 1% normal goat serum (NGS; DakoCytomation) of FITC-conjugated anti–mouse IgG (Fab specific; Sigma-Aldrich) for 10 minutes.

Flow cytometry

To measure the effect of CL administration on macrophages and dendritic cell (DC) numbers B6 mice were injected with the indicated concentration of CLs or PBSLs. Twenty-four hours later splenic single-cell suspensions were generated as described previously, and 10^6 cells were stained with 1 μg of anti-F/480 Alexa488 (clone CI:A3-1; Serotech), anti-CD11c allophycocyanin (APC; clone HL3; BD PharMingen), anti-CD86 PE (clone GL1; BD PharMingen), and anti-MHCII AF700 (clone M5/114.15.2; eBioscience).[23] To assay for apoptotic cell uptake 48 hours after CL administration mice were injected intravenously with 10^7 PKH26-labeled apoptotic cells in 200 μL of PBS. Thirty minutes and 2 hours after apoptotic cell injection splenocytes were stained with 1 μg of anti-CD68 Alexa488 (clone FA11; Serotech), anti-F4/80 APC (clone BM8; eBioscience), anti-CD86 PE (clone GL1; BD PharMingen), anti-CD11c Alexa488 (clone N418; eBioscience), anti-MHCII AF700 (clone M5/114.15.2; eBioscience), or anti-CCR7 APC (clone 4B12; eBioscience).

To measure T-cell proliferation B6.*CD45.1*$^+$ mice were treated with 167 μg of CLs or PBSLs. Twenty-four hours later 5×10^6 CFSE-labeled (Invitrogen) OTII splenocytes were adoptively transferred intravenously by lateral tail vein injection. Twenty-four hours after OTII transfer, mice were injected with 10^7 apoptotic Act-mOVA thymocytes in 200 μL of PBS intravenously. Three days after apoptotic cell transfer the spleen was collected, and proliferation was assessed by flow cytometry. To visualize the adoptively transferred OTII cells 5×10^6 splenocytes were stained with 2.5 μg of anti-CD45.2 AF700 (clone 104; eBioscience) and anti-CD4 peridinin chlorophyll protein complex (clone RM4.5; BD PharMingen).

For flow cytometric analysis $\geq 10^5$ (10^6 in the case of adoptive OTII transfer) events were collected on a FACSCanto flow cytometer (BD Bioscience), and all results were analyzed with FlowJo software (TreeStar).

Immunofluorescence and immunohistochemistry

To assay for immune deposits kidneys were embedded in Tissue-Tek OCT compound (Sakura) and snap frozen. Sections (5 μm) were air-dried, fixed with cold acetone, and stained with a 1:200 dilution in PBS plus 1% NGS of FITC-conjugated anti–mouse IgG (Sigma-Aldrich).

For MARCO and B220 staining spleens were fixed in acetone, and 5-μm sections were incubated with a 1:50 dilution of anti-MARCO FITC (clone ED31; Serotec) and a 1:150 dilution of anti-B220 biotin (clone RA3-6B2; BD PharMingen) followed by incubation with alkaline phosphatase–conjugated anti-FITC and HRP-conjugated antibiotin (Serotech) antibodies. After extensive washing in PBS the antibody staining was visualized with a 3–3′-diaminobenzidine and 5-bromo-4-chloro-3-indolyl-phosphate 4-nitroblue tetrazolium chloride substrate kit (Vector Laboratories).

To analyze localization of apoptotic cells in the spleen syngeneic thymocytes were prepared and stained with 2μM PKH26 (Sigma-Aldrich) before induction of apoptosis. Cells (10^8) were injected intravenously into B6 mice. Spleens were collected 2 hours later and frozen in OCT. Six-μm-thin sections were cut in a cryostat microtome. After overnight drying, the slides were fixed in acetone and stored at −75°C. Before staining, slides were blocked with 5% NGS (Dako Cytomation) and 4% BSA in PBS. The following antibodies were used: anti-MARCO FITC (clone ED31), anti–SignR1 Alexa488 (clone ER-TR9), anti-MOMA2 Alexa488 (clone MOMA-1; Serotec), and anti–B220 APC (clone RA3-6B2; BD PharMingen).

In one set of experiments mice were injected intravenously with 167 μg/kg CLs followed 48 hours later with 5×10^8 fluorescein-labeled polystyrene beads (Polysciences) 1 μm in diameter. Two hours after injection spleens were collected and examined for particle localization by confocal microscopy. Fluroescent images were collected using a Leica DM IRBE confocal laser scanning microscope (Leica Microsystems) equipped with 1 argon and 2 HeNe lasers, using an HC PL APO lens at 20×/0.70 IMM CORR and 40×/1.3 oil and 90% glycerol (MP Biomedicals). Brightfield images were collected using a Nikon Eclipse 90i microscope (Nikon) using a Nikon Planflor lens at 20×/0.50 IMM CORR. Images were processed with Adobe Photoshop CS3 Extended 10.0.1 (Adobe Systems).

Pathology

Paraffin kidney sections (5 μm) were stained with Periodic acid Schiff reagent and H&E. Glomerulonephritis was scored as described previously.[24] The lesions graded included thickening of the mesangium, noticeable increases in both mesangial and glomerular cellularity with/without

superimposed inflammatory exudates and capsular adhesions, glomerulosclerosis, and cast formation. Scoring was performed on ≥ 200 glomeruli in a 40× field per kidney.

Image and statistical analysis

Image analysis for PKH26 localization was done with NIH IMAGEJ software Version 1.41. Means, SD, and unpaired Student *t* test results were used to analyze the data. When comparing 2 groups, a P value $> .05$ was considered to be significant. Survival data were analyzed with Kaplan-Meier survival plots followed by the log-rank test.

Results

Low-dose CLs intravenously specifically deplete MZM.

CLs are often used for phagocyte depletion.[22] The depletion is considered near complete in the spleen and liver when doses > 40 mg/kg are administered intravenously. However, Aichele et al[4] reported that limited-dose CLs specifically target MZM populations. To assess this we injected various doses of CLs or control liposomes intravenously and 24 hours later enumerated F4/80$^+$ macrophages and CD11c$^+$ DC numbers by FACS. Injection of 1 mg (ie, 40 mg/kg) of CLs intravenously reduced splenic DC numbers by 98% and F4/80$^+$ macrophage numbers by 85% (supplemental Figure 1A). In contrast, intravenous administration of 167 μg (6.5 mg/kg) of CLs or lower doses did not affect overall splenic DC or macrophage percentages. Moreover, although 1 mg of CLs altered MHCII and CD86 expression on the remaining DC and macrophage populations, respectively, injection of lower amounts of CLs had no effect on MHCII or CD86 in either cell compartment (supplemental Figure 1B).

When splenic sections were stained with markers for MZMs (ie, MARCO and MOMA-1), we found administration of 167 μg or 83 μg of CLs depleted MZMs detectible by immunohistochemistry (supplemental Figure 1C), whereas further reduction of the CL dose to 42 μg (1.6 mg/kg) had no effect (supplemental Figure 1C). Depletion was not associated with changes in lymphocyte localization or follicular structure, suggesting low-dose CL administration specifically targets MZMs. Thus, we used these dosages of CLs to examine the effect of MZM removal on the splenic response to apoptotic material.

MZM depletion alters apoptotic cell trafficking in the spleen

In general, apoptotic cells entering the spleen from circulation localize to the MZ and RP with gradual accumulation by DC-mediated transport into the WP.[25,26] Accordingly, control spleens showed localization of labeled apoptotic material primarily in the MZ and to a lesser degree in the RP. Costaining showed that most material was in close proximity to MARCO$^+$ MZMs (Figure 1A).[11] Strikingly, in mice depleted of MZMs, there was significant accumulation of apoptotic material in the periarteriolar lymphoid sheath (PALS) (Figure 1A lower panels). This change was apparent by 2 hours after injection and remained so for up to 6 hours (not shown), suggesting lack of MZMs significantly alters apoptotic cell localization. Semiquantitative analysis of the PALS indicated that MZM-depleted spleens had a greater accumulation of apoptotic material as assessed by overall fluorescence intensity. Moreover, the average size of the accumulated apoptotic cell clusters was 3-fold larger in MZM-depleted spleens than for controls (Figure 1B), an indication of significant alteration in apoptotic cell accumulation in the WP.

RP macrophages increase phagocytosis of apoptotic cells in the absence of MZMs

MAdCAM-1$^+$ endothelial cells lining the marginal sinus provide a barrier preventing inappropriate follicular access to blood-borne products and regulating lymphocyte homing.[27-29] Thus, it is unlikely that apoptotic cell accumulation in the PALS would occur by a passive fashion if the MAdCAM-1$^+$ layer were intact. Kraal et al[27] observed that injection of high-dose CLs disrupted splenic MAdCAM-1$^+$ cell localization. Similarly, we found that high-dose (ie, 1 mg) CLs altered the localization of MadCAM-1$^+$ cells with more diffuse staining, suggesting mobilization, primarily into the follicle (Figure 1C). In contrast, there was no change in the appearance of MAdCAM-1$^+$ cells surrounding the sinus when low-dose (ie, 167 μg or 83 μg) CLs was administered, suggesting PALS accumulation of apoptotic cells was not because of disruption of the endothelial cell layer.

To further test if MZM depletion altered particulate antigen trafficking in a general fashion we injected MZM-depleted animals with fluorescein-labeled 1-μm particles and examined localization 2 hours after injection. In controls the particles localized almost exclusively to the MZMs with little to no accumulation in either the RP or PALS (Figure 1D). In MZM-depleted spleens, the particles were diffusely localized in the RP but were still absent from the WP (Figure 1E). Thus, MZM absence does not disrupt the integrity of the MZ barrier to passive material transport into the WP.

Because macrophages make up the majority of RP phagocytes, we examined apoptotic cell uptake in this population 30 minutes and 2 hours after administration. In PBSL-treated animals the percentage of CD68$^+$F4/80$^+$ macrophages that phagocytosed labeled thymocytes was low and never increased to > 5% (Figure 2A-B). In contrast, after MZM depletion there was a 3-fold increase in phagocytosis of apoptotic cells by macrophages 30 minutes after transfer (Figure 2A) and increasing to 40% 2 hours after transfer (Figure 2A-B). Moreover, the relative apoptotic cell label in PKH26$^+$ macrophages was 10-fold higher after MZM depletion than for controls (Figure 2C), suggesting a higher phagocytic activity.

Surface CD86 was increased overall in CD68$^+$F4/80$^+$ macrophages; however, when the data were parsed on the basis of apoptotic cell costaining, we found increased CD86 was confined to macrophages that had phagocytosed apoptotic cells (Figure 2D). Moreover, in MZM-depleted conditions there was a slight, but highly significant, increase in CD86 MFI compared with PBSL controls.

MHCII expression was not changed in CD68$^+$F4/80$^+$ macrophages from control animals regardless of whether they had taken up apoptotic material. In contrast, in MZM-deficient mice, apoptotic cell phagocytosis increased MHCII expression (Figure 2D), suggesting rapid alteration in macrophage phenotype. Moreover, it is an indication that MZM function affects the clearance of apoptotic material in both a qualitative and quantitative manner.

DC-mediated transport of apoptotic cells from the RP to the PALS is associated with increased expression of the chemokine receptor CCR7, facilitating follicular localization.[30,31] We reasoned that, if macrophages are responsible for the altered localization of apoptotic cells to the PALS, they might experience similar increases in CCR7 expression after apoptotic cell uptake. When CCR7 was examined, we found in control mice that apoptotic cell phagocytosis by CD68$^+$F4/80$^+$ macrophages slightly increased CCR7 expression over baseline (Figure 2D). However, after MZM depletion CCR7 staining increased 2-fold over baseline values.

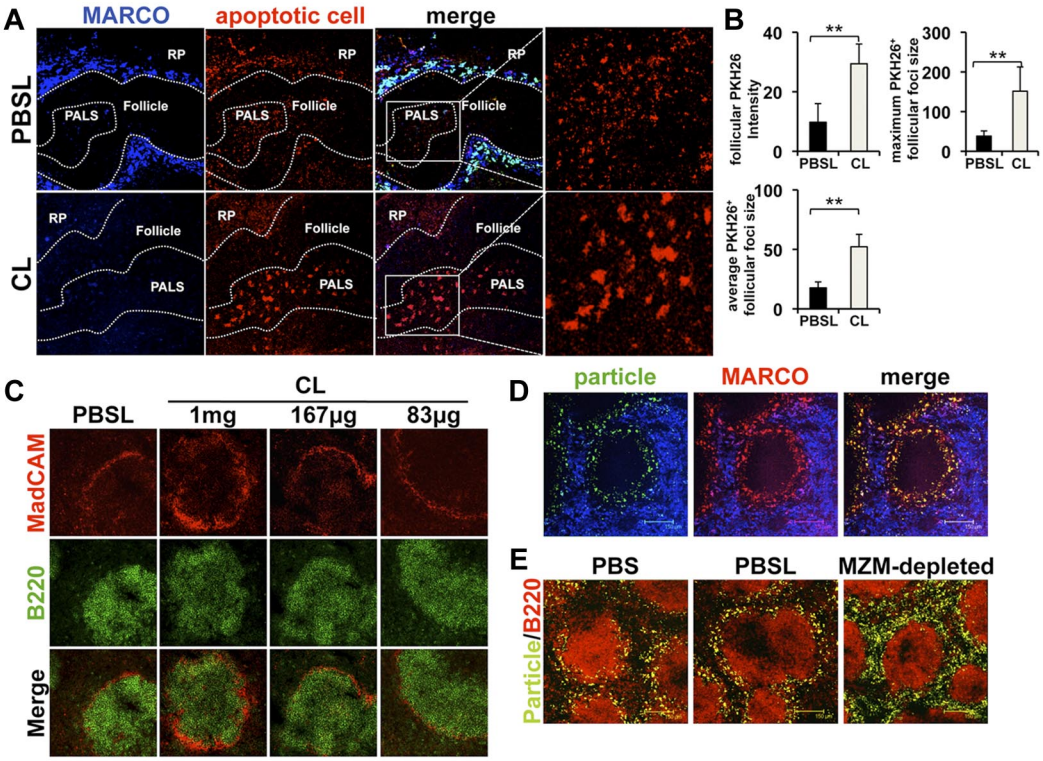

Figure 1. Marginal macrophage depletion alters apoptotic cell localization without disrupting the marginal sinus. (A) Eight- to 12-week-old female B6 mice were injected intravenously with 167 μg of CLs or an equivalent amount of PBSLs in 200 μL final volume. Forty-eight hours later the mice were injected intravenously with 10^8 PKH26-labeled apoptotic thymocytes. Two hours after apoptotic cell injection the spleen was removed, and 5-μm frozen sections were stained with antibodies against MARCO. The sections were examined by microscopy for localization of the apoptotic cells within the spleen. RP indicates red pulp; and PALS, periarteriolar lymphoid sheath. CL-N = 7 mice, PBSL-N = 4 mice. (B) Image analysis of PHK26 fluorescence in the PALS of MZM-depleted and control mice. Y-axis values for size are image pixels and are representative for relative signal size. Bars represent the mean values for CL-N = 7 mice, PBSL-N = 4 mice. $^{**}P < .01$ as determined by the unpaired Student *t* test. (C) B6 mice, as in panel A, were injected with the indicated amounts of CLs or an amount of PBSLs equivalent to the highest dose of CLs administered intravenously. Forty-eight hours later spleens were collected, and 10-μm frozen sections were stained with antibodies against MadCAM-1 (red) and B220 (green). Images are representative of 5 mice/group. (D) B6 mouse splenic section (n = 3 mice/group) 2 hours after injection with 5×10^8 fluorescent microparticles administered as described in "Immunofluorescence and immunohistochemistry" and stained with antibodies against MARCO (red) and F4/80 (blue). (E) B6 mice (n = 3 mice/group) were depleted of MZMs, and microparticles were injected as described in panel D. Two hours after injection spleens were collected, and sections were examined for particle localization and stained with antibodies against B220 (red) to visualize the follicle. All images are 2-μm confocal pictures captured as described in "Immunofluorescence and immunohistochemistry" and are representative for each group. Image magnification 20×. These experiments were repeated at least twice with similar results.

Coupled with increased overall phagocytosis, this suggests a significant portion of RP macrophages may reposition themselves, migrating to the PALS in an apoptotic cell–induced, CCR7-dependent manner. To examine macrophage localization we stained splenic sections for MOMA-2, a marker for tissue macrophages.[32] In PBSL-treated animals MOMA-2 staining was apparent in both RP and the PALS (Figure 2E). Moreover, as in Figure 2A, most apoptotic cells localized to the MZ with a prominent localization near the MZ sinus (Figure 2E arrow). After MZM depletion MOMA-2 staining was relatively unchanged with the exception of large clusters of MOMA-2^+ cells in the PALS. Moreover, MOMA-2 staining overlaid with apoptotic cell localization. further suggesting macrophage-mediated transport to the PALS.

We hypothesized that the absence of MZMs may influence the cytokine response to apoptotic cell administration. To test this we examined splenic and serum cytokine profiles 4 and 18 hours after apoptotic cell injection. It is well described that apoptotic cell exposure leads to increased TGF-β1 synthesis. We found this to be the case because apoptotic cell injection in controls led to a large increase in TGF-β 18 hours after injection (Figure 3A). Apoptotic cells also increased TNF-α 4 hours after injection. This is in agreement with some reports suggesting apoptotic cell uptake can induce limited proinflammatory cytokine production.[33-35] In contrast, MZM depletion reduced TGF-β1 induction after apoptotic cell injection coupled with increased IL-6 and IL-12 levels (Figure 3A). We found no changes in IFN-γ, IL-10, IL-13, or IL-17 compared with control mice (not shown). The increase in proinflammatory cytokines was not due to nonspecific CL-mediated conditioning because the cytokine profile in CL-injected controls was unchanged compared with PBSL-treated mice (Figure 3A). Thus, taken together, the data suggest that the lack of MZMs significantly altered apoptotic cell interactions with other phagocytes in the RP, notably $CD68^+F4/80^+$ macrophages, resulting in aberrant uptake, activation, and localization of macrophages associated with apoptotic material trafficking to the lymphoid WP.

Although macrophages are not generally considered efficient antigen-presenting cells, Okamoto et al[36] reported that $F4/80^+$ macrophages are capable of promoting T-cell reactivity to nucleosomal antigens. Moreover, they suggested macrophages are important in the development of systemic autoimmunity by antigen presentation. On the basis of our observations we reasoned that the increased apoptotic cell uptake by $CD68^+F4/80^+$ macrophages, coupled with increased activation and localization to the lymphoid area of the spleen, might increase apoptotic cell–associated antigen presentation to lymphocytes, resulting in enhanced immune reactivity. To test this we depleted mice of MZMs followed by transfer of CFSE-labeled OVA-specific OTII $CD4^+$ T cells. Twenty-four hours after T-cell transfer we injected OVA-expressing apoptotic

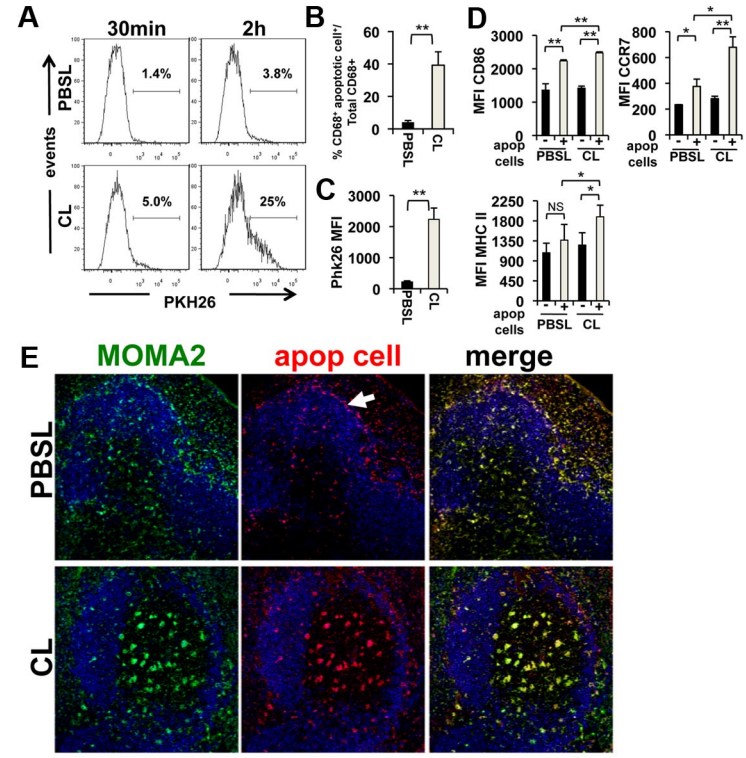

Figure 2. Apoptotic cell phagocytosis is increased in CD68$^+$F4/80$^+$ RP macrophages in the absence of MZMs. (A) Eight- to 12-week-old female B6 mice were injected intravenously with 167 μg of CLs or an equivalent amount of PBSLs. Forty-eight hours later 10^7 PKH26-labeled apoptotic thymocytes were transferred intravenously, and at 30 minutes and 2 hours after apoptotic cell injection CD68$^+$F/480$^+$ macrophages were assessed for cell uptake. Histograms are representative for 5 mice/group enumerated in panel B. (C) Relative PKH26 fluorescence intensity for the CD68$^+$F/480$^+$PKH26$^+$ macrophage populations depicted in panel A 2 hours after apoptotic thymocyte administration. MFI indicates mean fluorescence intensity; n = 5 mice/group. (D) Relative expression of the surface antigens CD86, MHCII, and CCR7 was examined in CD68$^+$F4/80$^+$ macrophages by FACS analysis in mice treated as described in panel A at 2 hours after apoptotic cell injection. Values were parsed on the basis of PKH26 fluorescence, which was indicative of apoptotic cell phagocytosis. Bars represent the mean value of 5 samples ± SD. (E) Spleens from mice treated as in panel A were collected at 2 hours after apoptotic cell injection. Frozen sections (5 μm) were stained with antibodies against the macrophage marker MOMA2 and examined for localization of macrophages and apoptotic material by fluorescent microscopy. Arrow highlights area of apoptotic cell capture in the MZ zone in PBSL control spleens which is absent in CL-treated splenic sections. Images are representative for 3 mice/group. Image magnification 20×. All experiments were repeated multiple times with similar results. *$P < .05$ and **$P < .01$ as determined by the unpaired Student *t* test.

thymocytes and examined the T-cell proliferation. Under these conditions OTII T cells showed little response to apoptotic cell–associated antigen (Figure 3B-C). In contrast, after MZM depletion, OTII T cells proliferated vigorously 3 days after apoptotic Act-mOVA thymocyte transfer with ~ 70% of the OTII T cells having undergone cell division (Figure 3C), supporting the hypothesis that MZMs regulate the processing of apoptotic material within the spleen.

MZM loss accelerates autoimmune disease in mice prone to systemic lupus erythematosus

The data suggest a lack of MZM function might alter immune responsiveness to apoptotic cells, enhancing the ability to acquire and present antigen to T cells. Because this process may promote the development of autoimmunity, we examined the effect of MZM depletion on the development of serum autoreactivity in the B6.*fcgr2b*$^{-/-}$ lupus model. For this, we depleted MZMs by weekly injection of CLs, beginning at 4 weeks of age and examining autoreactivity in mice after 2 months. In B6.*fcgr2b*$^{-/-}$ mice measurable serum autoreactivity typically develops in females from 4-6 months of age.[23,37] In accordance with this, B6.*fcgr2b*$^{-/-}$ mice injected with PBSLs showed no evidence of serum ANA reactivity (Figure 4A), anti-dsDNA reactivity (Figure 4B), or increased immune complex (IC) deposition (Figure 4C) at 3 months of age. However, when MZMs were depleted, the mice showed evidence of autoimmunity, including positive ANA test, increased serum anti-dsDNA reactivity, and significant renal IC deposition (Figure 4A-C). Of interest was the fact that CL-mediated acceleration of autoimmunity onset only occurred with amounts of CLs affecting MZM numbers (supplemental Figure 1C), strongly suggesting that the acceleration of disease occurs because of the lack of MZM function.

To determine whether MZM depletion would compromise tolerance in wild-type mice, we repeated the experiment with the use of both B6.*fcgr2b*$^{-/-}$ mice and B6 mice, examining the development of serum autoreactivity over a period of 6 months. In SLE-prone (ie, B6.*fcgr2b*$^{-/-}$) mice the loss of MZMs greatly accelerated serum autoreactivity in agreement with our earlier experiments.

Here, control B6.*fcgr2b*$^{-/-}$ mice developed detectible anti-dsDNA IgG reactivity at 4 months after treatment (ie, 5 months of age), increasing to considerable autoreactivity by 6 months, in line with established disease progression for the strain. In contrast, MZM depletion significantly increased serum reactivity to dsDNA relative to controls at 4 months (OD^{450nm} 0.89 + 0.33 vs 0.51 + 0.06 for the CL and PBSL groups, respectively). This trend continued at 6 months with an ever-increasing difference between MZM-depleted and control animals (OD^{450nm} 1.6 + 0.45 vs 0.77 + 0.16 for the CL and PBSL groups, respectively; Figure 4D). Taken together, the data strongly suggest the lack of MZMs further compromises immune homeostasis in SLE-prone mice, contributing to disease development.

Contrary to the observations in SLE-prone mice, we found no evidence of autoimmunity in MZM-depleted B6 mice at any time during the course of the experiment (Figure 4D). This suggests that the lack of MZM function does not act in a dominant fashion to promote a loss of systemic tolerance, but disruption of MZM regulatory functions may act in an epistatic fashion, accelerating tolerance loss on susceptible backgrounds. These data are at odds with Denny et al[38] who reported that CL administration promoted autoimmunity in wild-type mice because of increased apoptosis of phagocytes. However, in other reports CL administration was shown to prevent autoimmune pathology in SLE-prone mice; thus, it is not clear from the literature what effect CL administration has on homeostasis and autoimmunity development. To examine the potential effect of CLs in the development of systemic autoimmune disease, we injected wild-type (B6) mice with CLs intravenously once a week for 6 months at high- and low-dose concentrations (ie, 1 mg, 167 μg, 83 μg, or PBSLs), examining the incidence of autoimmunity.

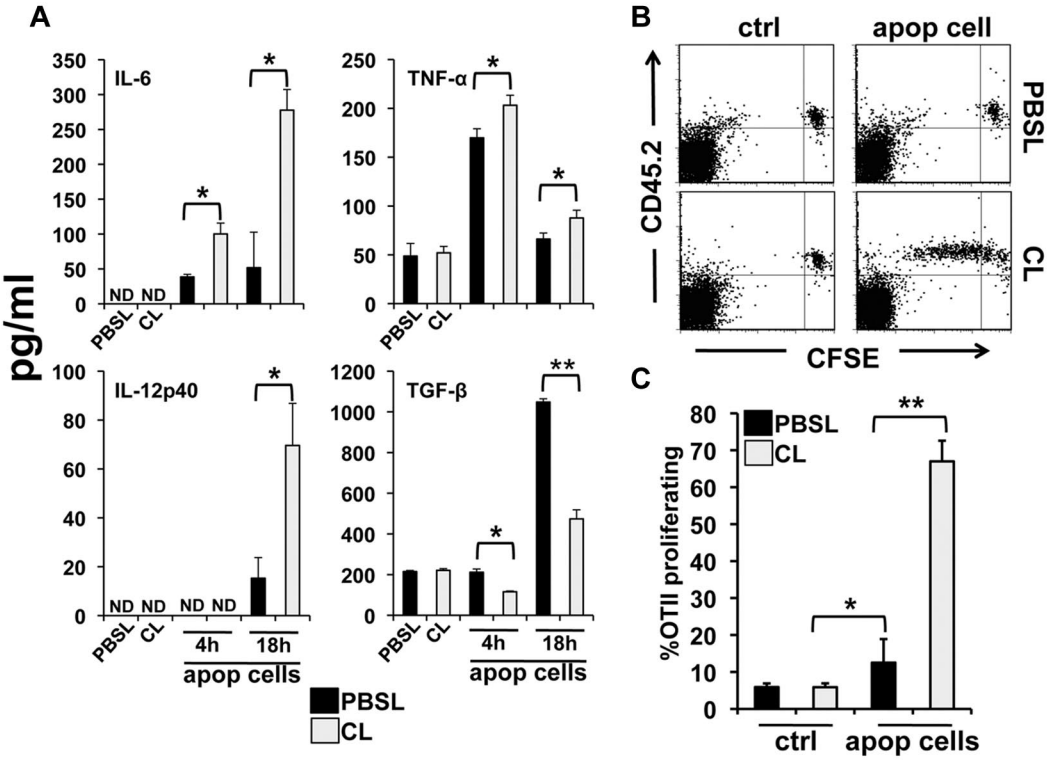

Figure 3. Lack of MZMs increases apoptotic cell–induced proinflammatory cytokines and enhances T-cell responsiveness to apoptotic cell–associated antigens. Eight- to 12-week-old female B6 mice were injected intravenously with 167 μg of CLs or an equivalent amount of PBSLs in a 200-μL final volume. Forty-eight hours later 5×10^7 apoptotic thymocytes were transferred intravenously. (A) Four and 18 hours after thymocyte injection serum was collected and assessed for the presence of IL-6, IL-12, IFN-γ, IL-10, IL-13, TNF-α, TGF-β1, and IL-17. Bars are mean values for 4 mice/group. CL and PBSL control groups are shown for the 18-hour time point. (B) Eight- to 12-week-old female B6.*CD45.1* mice were injected intravenously with 167 μg of CLs or an equivalent amount of PBSLs in a 200-μL final volume. Forty-eight hours later 5×10^6 CFSE-labeled splenocytes from CD45.2$^+$ OTII mice were transferred intravenously into CL0 and PBSL-treated animals. One day (ie, 24 hours) later 10^7 apoptotic thymocytes from OVA protein-expressing Act-mOVA mice were transferred by tail vein injection. Three days after apoptotic cell injection single-cell splenocyte suspensions were examined by FACS for the proliferation of the OTII CD4$^+$ T cells by virtue of CFSE diminution. Dot plots represent samples gated on the CD4$^+$ splenocyte population and stained with antibodies against CD45.2, identifying the transferred OTII CD4$^+$ T cells (n = 5 mice/group). (C) Graphic representation of the data presented in panel C**.** Bars in graphs represent the mean value for 5 mice ± SD; *$P < .05$ and **$P < .01$ as determined by the unpaired Student *t* test. ND indicates none detected. These experiments were repeated at least twice with similar results.

In agreement with our previous experiments, repeated administration of low-dose CLs did not affect basal serum autoreactivity, splenic architecture, or IC deposition in wild-type mice. However, in mice receiving chronic high-dose CLs (1 mg/injection), we detected striking levels of anti-dsDNA antibodies (Figure 5A), as well as 50% mortality over 5 months (Figure 5B). We also found increased IC deposition in the glomeruli (Figure 5C), whereas low doses of CLs remained at background levels. Thus, the data would suggest that high-dose CLs can generate significant autoimmunity in healthy mice, whereas low-dose CLs has no affect on overall immune homeostasis.

MZM loss renders wild-type animals susceptible to apoptotic cell–driven autoimmunity

Although the loss of MZMs is insufficient for development of spontaneous autoimmunity, our results clearly showed that MZM function significantly affects how apoptotic antigens are processed in the spleen. It is possible that inherent redundancies in peripheral regulatory mechanisms would prevent spontaneous tolerance breakdown in the event one or perhaps even multiple mechanisms of regulation fail. However, as we have shown in SR-A/MARCO double KO mice and in CD1d$^{-/-}$ mice[11,39] that have apparently intact tolerance, mice can be driven to develop autoreactivity by increased-load apoptotic cell administration. Thus, we conducted experiments to determine whether this was the case for MZM-depleted mice. For this MZM-depleted B6 mice were injected 2 times weekly with 10^7 apoptotic thymocytes, and serum autoreactivity to dsDNA was monitored. We found that there was no initial increase in autoantibody reactivity over the baseline values; however, by month 3 there was increased reactivity to dsDNA in MZM-deficient animals relative to control mice (Figure 6A). Moreover, at later time points the autoreactivity increased substantially, suggesting an acceleration of autoimmunity and an increasing loss of immune regulation in MZM-depleted mice challenged with apoptotic material. Unexpectedly, we also observed significantly increased mortality in MZM-depleted mice chronically exposed to high-load apoptotic cells ($P = .02$; Figure 6B). The mortality was not because of CL administration, because CL treatment alone did not increase mortality. Similarly, we did not observe any mortality in mice injected with control liposomes (Figure 6B).

In murine models of systemic autoimmunity the kidney is the most frequent target organ. When the kidneys of MZM-depleted mice receiving chronic apoptotic cell injections were examined, we found significant evidence of pathology (Figure 6D). All mice had prominent perivascular and periglomerular infiltrates, mesangial thickening and hyperplasia, crescent formation, and evidence of tubular atrophy (Figure 6Div-v). Further, the glomeruli had noteworthy IC deposition (Figure 6Dvi). In contrast, the control groups had no evidence of pathologic alteration or increased IC in the kidney (Figure 6Di-iii). This was reflected in the pathology score in which MZM-depleted mice receiving apoptotic cells had significant

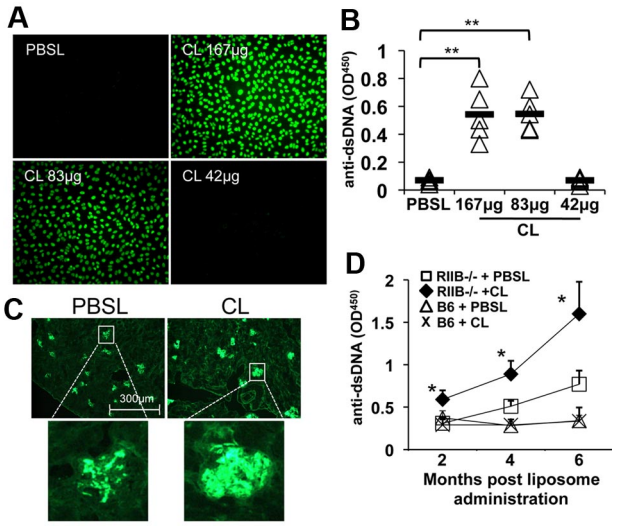

Figure 4. In the absence of MZMs systemic autoimmunity is accelerated in SLE-prone mice. Four-week-old female lupus-prone B6.*fcgr2b*$^{-/-}$ mice were injected with the indicated amounts of CLs in a final volume of 200 μL once a week for a period of 2 months. At the experimental end point sera was collected and assessed for the spontaneous development of serum ANA reactivity (A) or IgG autoantibodies against dsDNA (B) as described in "Autoantibody detection." (C) Kidney from female B6.*fcgr2b*$^{-/-}$ mice treated as in panel A with 167 μg of CLs or an equivalent amount of PBSLs were snap-frozen, and 5-μm sections were stained with anti–mouse IgG FITC to determine the extent of IgG immune complex deposition. Image magnification 20×. (D) Four-week-old female B6 and B6.*fcgr2b*$^{-/-}$ mice were intravenously administered 167 μg of CLs or equivalent PBSLs once a week for a period of 6 months. Sera were collected at the indicated time points and assessed for anti-dsDNA IgG reactivity as described. For all experiments, n = 5 mice/group; $^{*}P < .05$ and $^{**}P < .01$ as determined by the unpaired Student *t* test. These experiments were repeated at least twice with similar results.

inflammatory alteration in the kidney, whereas none of the control animals showed evidence of significant pathology (Figure 6C). Thus, it is probable that the combination of MZM deficiency coupled with the increased presence of apoptotic cells was sufficient to disrupt immune homeostasis, resulting in autoimmunity, renal pathology, and increased mortality.

Discussion

The effects of cell death on the immune system are complex and are regulated to a significant degree by physiologically and temporally mediated factors.[40,41] The spleen may be a site for generation of regulatory responses to peripheral antigens because splenectomy can abrogate tolerance to antigens applied either systemically or in immune-privileged sites.[42,43] How apoptotic cell–associated suppression is induced is not understood, although apoptotic material entering the spleen localizes to the MZ and RP so presumably regulatory functions would initiate there. In this vein several groups have reported that MZ CD8^{+}DCs phagocytose apoptotic cells by mechanisms involving direct recognition of the apoptotic cell and secondary opsonin,[25,26,43,44] resulting in migration to the PALS and induction of tolerance by T-cell anergy and T^{reg} cell–mediated mechanisms. However, observations by our laboratory and others that apoptotic cells are found in direct association with MZMs and the fact that apoptotic cells can elicit autoimmunity in scavenger receptor-deficient mice suggest that MZMs play a role in the response to apoptotic material.

To examine this we used a depletion technique that took advantage of the specialized features of MZMs, namely anatomical positioning, high-phagocytic capacity, and affinity for lipids by scavenger receptor expression to target them for removal by CLs. In the absence of MZMs there were no observable changes in splenic architecture. However, apoptotic cell localization was significantly altered in the absence of MZMs. Within 30 minutes of injection we found significant accumulation of material in the PALS. This accumulation increased ≤ 2 hours after transfer and was maintained for ≥ 5-6 hours, indicating a noteworthy disruption in trafficking patterns (as seen in Figure 1). Because the follicle is a protected structure, we reasoned that active uptake and transport may account for this. Indeed, we found that CD68^{+}F4/80^{+} macrophages ingested significant amounts of apoptotic material in the absence of MZMs. Increased expression of MHCII and CD86 suggests that apoptotic cell uptake is associated with

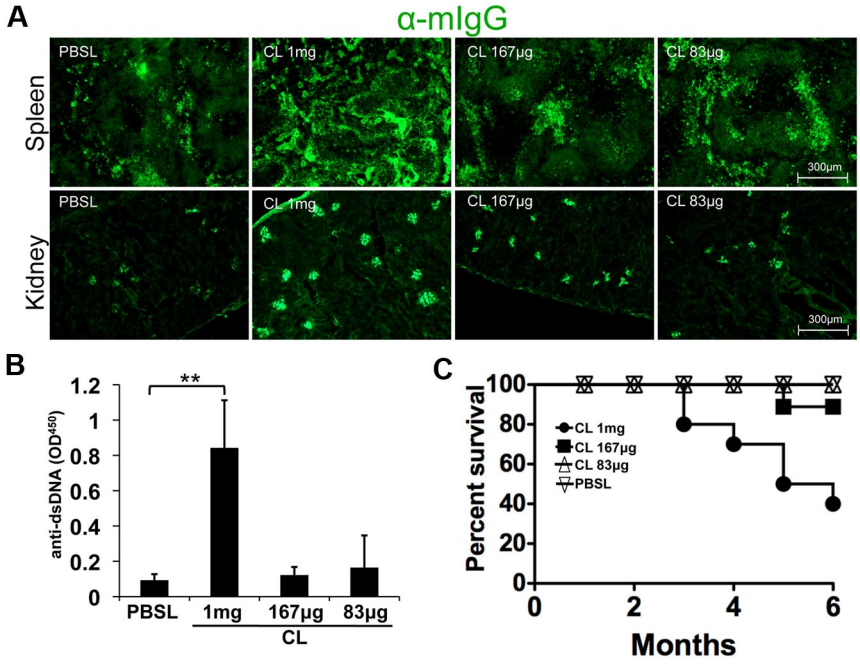

Figure 5. Chronic high-dose CLs induce spontaneous autoimmune disease in wild-type mice. Eight-week-old female C57Bl/6 mice were injected with the indicated amounts of CLs once a week for a period of 6 months. (A) frozen spleen and kidney sections (5 μm) from mice treated for 6 months as indicated were stained with anti–mouse IgG FITC to examine spleen structure, IgG production (spleen), and immune complex deposition (kidney). Image magnification 20×. (B) Sera were collected from mice after 5 months of chronic administration of the indicated amounts of CLs and examined for IgG reactivity to dsDNA by ELISA as described. (C) Survival curve for mice treated as described over the course of a 6-month exposure to CLs or PBSLs. For all experiments, n = 10 mice/group; $^{**}P < .01$ as determined by the unpaired Student *t* test. This experiment was repeated twice with similar results.

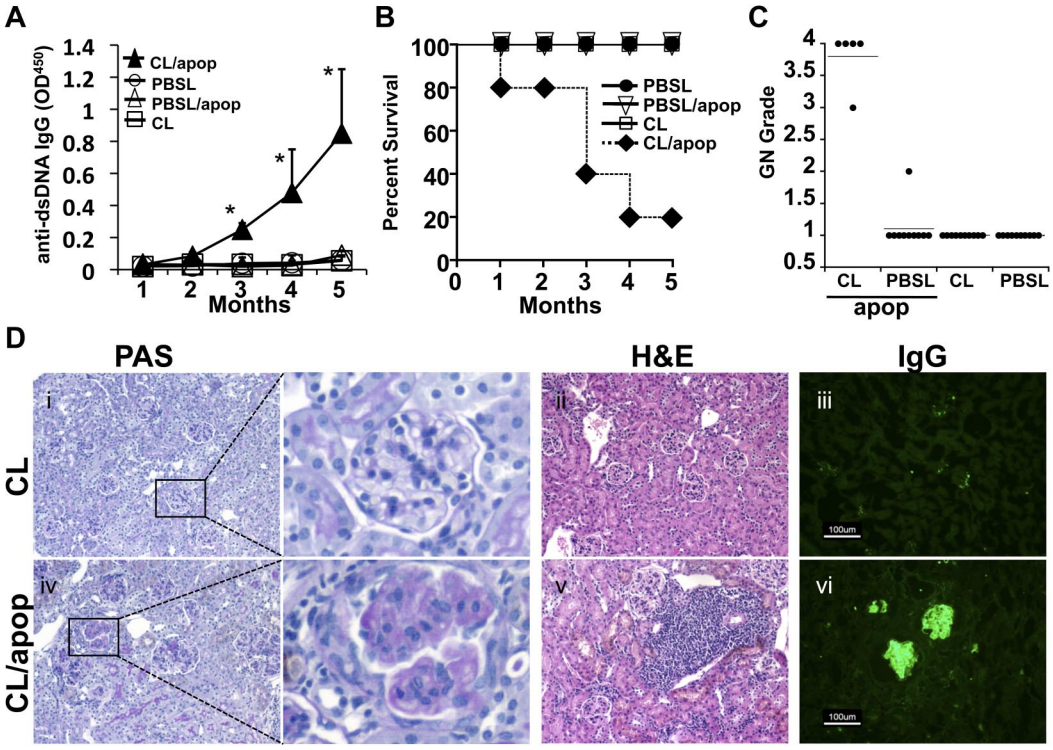

Figure 6. Absence of MZMs causes a loss of tolerance after repeated exposure to apoptotic cells. Eight-week-old female B6 mice were injected with 167 μg of CLs or an equivalent amount of control liposomes once a week for a period of 5 months. Some groups received intravenously 2 times weekly injections of 10^7 apoptotic thymocytes as indicated. (A) Sera were collected once monthly for a period of 5 months and examined for anti-dsDNA IgG reactivity as described elsewhere. (B) Survival curves for mice treated as described in panel A; n = 10 mice/group; $^*P < .05$ as determined by the unpaired Student *t* test. (C) Kidney pathology score. H&E-stained renal sections from the from the groups described in panel A were collected at 5 months and scored for pathologic alteration as described in "Pathology." GN indicates glomerulonephritis; n = 10 mice for all groups except CL/apop in which organs from 5 mice were examined. (D) Histology and immune complex deposition. Periodic acid Schiff reagent and H&E images from the mice examined in panel C (Di,ii,iv,v). (Diii,vi) Representative frozen renal sections from the groups indicated were stained for the presence of mouse IgG as described in "Pathology." All images are 20× magnification. These experiments were repeated twice with similar results.

increased activation, perhaps accounting for the changes in splenic position. Moreover, immunofluorescent staining of spleen sections showed colocalization of the macrophage marker MOMA-2 and apoptotic cells, suggesting that a primary way they reach the PALS is by macrophage-dependent mechanisms.

The data imply apoptotic cell–associated antigens are poor inducers of antigen-specific T-cell activation in vivo when $< 10^7$ apoptotic cells are administered. This was changed dramatically by the abrogation of MZMs, whereby we saw significant T-cell proliferation. This is probable because of increased apoptotic cell uptake by and maturation of $CD68^+F4/80^+$ macrophages, resulting in increased antigen presentation and access within the WP. Although macrophages are regarded as poor mediators of T-cell activation, Okamoto et al[36] demonstrated that they are important for the activation of autoreactive T cells. Moreover, removal of $F4/80^+$ splenic macrophages retarded development of autoantibodies and autoimmune pathology in $NZB/NZWF_1$ mice, suggesting a role in the cause of murine lupus.

Further, we found that long-term removal of MZMs accelerated autoimmunity in lupus-prone mice. Yet, the lack of autoimmunity in B6 mice deficient in MZMs indicates that regulatory mechanisms enforced by MZMs do not have a dominant effect on systemic immune homeostasis. This is not surprising because the consequences of tolerance breakdown are severe; thus, there is probably a large amount of redundancy if one (or perhaps several) of these mechanisms is deficient. However, the loss of MZMs does compromise immunoregulation because chronic exposure to increased-load apoptotic cells resulted in the development of significant autoimmunity associated with increased mortality in B6 mice. Nevertheless, although our data show a clear alteration of splenic interaction with apoptotic material in MZM-deficient mice, contributing to autoimmune disease development, we cannot rule out the involvement of other cell types to the pathologic process. In particular, mesangial cells could be affected by CL administration, affecting glomerular biology and contributing to autoimmunity. Thus, the role for mesangial cells in this process will need clarification in future studies.

Significantly, our study showed in the absence of MZM-mediated capture/processing that apoptotic cells can incite a proinflammatory response in vivo. This is surprising on the basis of the large wealth of data indicating that apoptotic cells are by design immunosuppressive. However, the effect of apoptotic material on the immune system is probably predicated on temporal and anatomically regulated factors not easily reproduced ex vivo. Thus, the act of apoptosis alone may not be sufficient in and of itself for an immunoregulatory response requiring proper cell and spatial interactions that are compromised in the absence of MZMs.

How MZMs influence apoptotic cell–mediated immune regulation is not known. Although the fact that MZM absence delays apoptotic cell clearance[17] suggests a direct capture mechanism. However, MZM numbers are low in the spleen with estimates suggesting they comprise $< 1\%$ splenocytes,[45] indicating other active mechanisms must be involved. In this vein, the anti-inflammatory properties of intravenous immunoglobulin appear to manifest by interaction with SIGNR1 expressed by MZMs.[46,47] The remarkable aspect of intravenous immunoglobulin suppression is that it appears to be systemic acting distal to the spleen.[47] Thus,

MZMs may regulate inflammation and tolerance by the release of soluble factors that can act locally and systemically

In conclusion, our data suggest that MZMs play an important role in the regulation of splenic apoptotic cell antigen processing. Although we do not yet know precisely what these mechanisms are, increased understanding of this process will yield insights leading to better treatment of systemic autoimmune and autoinflammatory disease. Moreover, these findings may have implications for macrophage-mediated regulation in a more general sense that could have broad repercussions in infection, inflammation, and innate immunity.

Acknowledgments

We thank Sushama Wakade for her expert technical assistance, Dr Phillip Chandler for assistance with the in vivo studies, and Dr Andrew Mellor for his comments on the manuscript.

This work was supported by an intramural grant from Georgia Health Sciences University (T.L.M.) and by grants from The Lupus Research Institute (T.L.M.), the Swedish Research Council (M.C.I.K.), the Swedish Medical Society (M.C.I.K.), King Gustaf V's 80-years foundation (M.C.I.K.), the Magnus Bergvall foundation (M.C.I.K.), and the Swedish Rheumatism Association (M.C.I.K.).

Authorship

Contribution: T.L.M. designed experiments, conducted experimental procedures, analyzed the data, and wrote the manuscript; Y.C. and B.R. conducted experimental procedures and analyzed the data; N.v.R. provided reagents critical to the experiments; and M.C.I.K. designed experiments and analyzed the data.

Conflict-of-interest disclosure: The authors declare no competing financial interests.

Correspondence: Tracy L. McGaha, Immunotherapy Center, CN4143, Georgia Health Sciences University, 1120 15th St, Augusta, GA 30912; e-mail: tmcgaha@georgiahealth.edu.

References

1. Kraal G, Mebius R. New insights into the cell biology of the marginal zone of the spleen. *Int Rev Cytol.* 2006;250:175-215.
2. Kraal G, Janse M. Marginal metallophilic cells of the mouse spleen identified by a monoclonal antibody. *Immunology.* 1986;58(4):665-669.
3. Dijkstra CD, Van Vliet E, Dopp EA, van der Lelij AA, Kraal G. Marginal zone macrophages identified by a monoclonal antibody: characterization of immuno- and enzyme-histochemical properties and functional capacities. *Immunology.* 1985;55(1):23-30.
4. Aichele P, Zinke J, Grode L, Schwendener RA, Kaufmann SH, Seiler P. Macrophages of the splenic marginal zone are essential for trapping of blood-borne particulate antigen but dispensable for induction of specific T cell responses. *J Immunol.* 2003;171(3):1148-1155.
5. Gorak PM, Engwerda CR, Kaye PM. Dendritic cells, but not macrophages, produce IL-12 immediately following Leishmania donovani infection. *Eur J Immunol.* 1998;28(2):687-695.
6. Seiler P, Aichele P, Odermatt B, Hengartner H, Zinkernagel RM, Schwendener RA. Crucial role of marginal zone macrophages and marginal zone metallophils in the clearance of lymphocytic choriomeningitis virus infection. *Eur J Immunol.* 1997;27(10):2626-2633.
7. Phillips R, Svensson M, Aziz N, et al. Innate killing of Leishmania donovani by macrophages of the splenic marginal zone requires IRF-7. *PLoS Pathog.* 6(3):e1000813.
8. Hughes DA, Fraser IP, Gordon S. Murine macrophage scavenger receptor: in vivo expression and function as receptor for macrophage adhesion in lymphoid and non-lymphoid organs. *Eur J Immunol.* 1995;25(2):466-473.
9. Kraal G, van der Laan LJ, Elomaa O, Tryggvason K. The macrophage receptor MARCO. *Microbes Infect.* 2000;2(3):313-316.
10. Platt N, Suzuki H, Kurihara Y, Kodama T, Gordon S. Role for the class A macrophage scavenger receptor in the phagocytosis of apoptotic thymocytes in vitro. *Proc Natl Acad Sci U S A.* 1996;93(22):12456-12460.
11. Wermeling F, Chen Y, Pikkarainen T, et al. Class A scavenger receptors regulate tolerance against apoptotic cells, and autoantibodies against these receptors are predictive of systemic lupus. *J Exp Med.* 2007;204(10):2259-2265.
12. Platt N, Suzuki H, Kodama T, Gordon S. Apoptotic thymocyte clearance in scavenger receptor class A-deficient mice is apparently normal. *J Immunol.* 2000;164(9):4861-4867.
13. Rogers NJ, Lees MJ, Gabriel L, et al. A defect in Marco expression contributes to systemic lupus erythematosus development via failure to clear apoptotic cells. *J Immunol.* 2009;182(4):1982-1990.
14. Fadok VA, Bratton DL, Konowal A, Freed PW, Westcott JY, Henson PM. Macrophages that have ingested apoptotic cells in vitro inhibit proinflammatory cytokine production through autocrine/paracrine mechanisms involving TGF-beta, PGE2, and PAF. *J Clin Invest.* 1998;101(4):890-898.
15. Huynh ML, Fadok VA, Henson PM. Phosphatidylserine-dependent ingestion of apoptotic cells promotes TGF-beta1 secretion and the resolution of inflammation. *J Clin Invest.* 2002;109(1):41-50.
16. Schildknecht A, Brauer S, Brenner C, et al. FoxP3+ regulatory T cells essentially contribute to peripheral CD8+ T-cell tolerance induced by steady-state dendritic cells. *Proc Natl Acad Sci U S A.* 2010;107(1):199-203.
17. Miyake Y, Asano K, Kaise H, Uemura M, Nakayama M, Tanaka M. Critical role of macrophages in the marginal zone in the suppression of immune responses to apoptotic cell-associated antigens. *J Clin Invest.* 2007;117(8):2268-2278.
18. Asano K, Miwa M, Miwa K, et al. Masking of phosphatidylserine inhibits apoptotic cell engulfment and induces autoantibody production in mice. *J Exp Med.* 2004;200(4):459-467.
19. Hanayama R, Tanaka M, Miyasaka K, et al. Autoimmune disease and impaired uptake of apoptotic cells in MFG-E8-deficient mice. *Science.* 2004;304(5674):1147-1150.
20. A-Gonzalez N, Bensinger SJ, Hong C, et al. Apoptotic cells promote their own clearance and immune tolerance through activation of the nuclear receptor LXR. *Immunity.* 2009;31(2):245-258.
21. Cohen PL, Caricchio R, Abraham V, et al. Delayed apoptotic cell clearance and lupus-like autoimmunity in mice lacking the c-mer membrane tyrosine kinase. *J Exp Med.* 2002;196(1):135-140.
22. van Rooijen N, van Kesteren-Hendrikx E. "In vivo" depletion of macrophages by liposome-mediated "suicide." *Methods Enzymol.* 2003;373:3-16.
23. McGaha TL, Sorrentino B, Ravetch JV. Restoration of tolerance in lupus by targeted inhibitory receptor expression. *Science.* 2005;307(5709):590-593.
24. McGaha TL, Karlsson MC, Ravetch JV. FcgammaRIIB deficiency leads to autoimmunity and a defective response to apoptosis in Mrl-MpJ mice. *J Immunol.* 2008;180(8):5670-5679.
25. Iyoda T, Shimoyama S, Liu K, et al. The CD8+ dendritic cell subset selectively endocytoses dying cells in culture and in vivo. *J Exp Med.* 2002;195(10):1289-1302.
26. Liu K, Iyoda T, Saternus M, Kimura Y, Inaba K, Steinman RM. Immune tolerance after delivery of dying cells to dendritic cells in situ. *J Exp Med.* 2002;196(8):1091-1097.
27. Kraal G, Schornagel K, Streeter PR, Holzmann B, Butcher EC. Expression of the mucosal vascular addressin, MAdCAM-1, on sinus-lining cells in the spleen. *Am J Pathol.* 1995;147(3):763-771.
28. Tanaka H, Hataba Y, Saito S, Fukushima O, Miyasaka M. Phenotypic characteristics and significance of reticular meshwork surrounding splenic white pulp of mice. *J Electron Microsc (Tokyo).* 1996;45(5):407-416.
29. Girkontaite I, Sakk V, Wagner M, et al. The sphingosine-1-phosphate (S1P) lysophospholipid receptor S1P3 regulates MAdCAM-1+ endothelial cells in splenic marginal sinus organization. *J Exp Med.* 2004;200(11):1491-1501.
30. Verbovetski I, Bychkov H, Trahtemberg U, et al. Opsonization of apoptotic cells by autologous iC3b facilitates clearance by immature dendritic cells, down-regulates DR and CD86, and up-regulates CC chemokine receptor 7. *J Exp Med.* 2002;196(12):1553-1561.
31. Ato M, Stager S, Engwerda CR, Kaye PM. Defective CCR7 expression on dendritic cells contributes to the development of visceral leishmaniasis. *Nat Immunol.* 2002;3(12):1185-1191.
32. Kraal G, Rep M, Janse M. Macrophages in T and B cell compartments and other tissue macrophages recognized by monoclonal antibody MOMA-2. An immunohistochemical study. *Scand J Immunol.* 1987;26(6):653-661.
33. Kurosaka K, Watanabe N, Kobayashi Y. Production of proinflammatory cytokines by resident tissue macrophages after phagocytosis of apoptotic cells. *Cell Immunol.* 2001;211(1):1-7.
34. Takahashi M, Kobayashi Y. Cytokine production in association with phagocytosis of apoptotic cells

by immature dendritic cells. *Cell Immunol.* 2003; 226(2):105-115.

35. Yamazaki T, Nagata K, Kobayashi Y. Cytokine production by M-CSF- and GM-CSF-induced mouse bone marrow-derived macrophages upon coculturing with late apoptotic cells. *Cell Immunol.* 2008;251(2):124-130.
36. Okamoto A, Fujio K, van Rooijen N, et al. Splenic phagocytes promote responses to nucleosomes in (NZB x NZW) F1 mice. *J Immunol.* 2008;181(8): 5264-5271.
37. Bolland S, Ravetch JV. Spontaneous autoimmune disease in Fc(gamma)RIIB-deficient mice results from strain-specific epistasis. *Immunity.* 2000;13(2):277-285.
38. Denny MF, Chandaroy P, Killen PD, et al. Accelerated macrophage apoptosis induces autoantibody formation and organ damage in systemic lupus erythematosus. *J Immunol.* 2006;176(4): 2095-2104.
39. Wermeling F, Lind SM, Jordo ED, Cardell SL, Karlsson MC. Invariant NKT cells limit activation of autoreactive CD1d-positive B cells. *J Exp Med.* 2010;207(5):943-952.
40. Green DR, Ferguson T, Zitvogel L, Kroemer G. Immunogenic and tolerogenic cell death. *Nat Rev Immunol.* 2009;9(5):353-363.
41. Wermeling F, Karlsson MC, McGaha TL. An anatomical view on macrophages in tolerance. *Autoimmun Rev.* 2009;9(1):49-52.
42. Griffith TS, Yu X, Herndon JM, Green DR, Ferguson TA. CD95-induced apoptosis of lymphocytes in an immune privileged site induces immunological tolerance. *Immunity.* 1996;5(1):7-16.
43. Ferguson TA, Herndon J, Elzey B, Griffith TS, Schoenberger S, Green DR. Uptake of apoptotic antigen-coupled cells by lymphoid dendritic cells and cross-priming of CD8(+) T cells produce active immune unresponsiveness. *J Immunol.* 2002; 168(11):5589-5595.
44. Morelli AE, Larregina AT, Shufesky WJ, et al. Internalization of circulating apoptotic cells by splenic marginal zone dendritic cells: dependence on complement receptors and effect on cytokine production. *Blood.* 2003;101(2):611-620.
45. Ato M, Nakano H, Kakiuchi T, Kaye PM. Localization of marginal zone macrophages is regulated by C-C chemokine ligands 21/19. *J Immunol.* 2004;173(8):4815-4820.
46. Anthony RM, Nimmerjahn F, Ashline DJ, Reinhold VN, Paulson JC, Ravetch JV. Recapitulation of IVIG anti-inflammatory activity with a recombinant IgG Fc. *Science.* 2008; 320(5874):373-376.
47. Anthony RM, Wermeling F, Karlsson MC, Ravetch JV. Identification of a receptor required for the anti-inflammatory activity of IVIG. *Proc Natl Acad Sci U S A.* 2008;105(50):19571-19578.